Stability analysis of the perfectly matched layer for the elastic wave equation in layered media

Kenneth Duru* Siyang Wang†

October 4, 2022

Abstract

In this paper, we present the stability analysis of the perfectly matched layer (PML) in two-space dimensional layered elastic media. Using normal mode analysis we prove that all interface wave modes present at a planar interface of bi-material elastic solids are dissipated by the PML. Numerical experiments in two-layer and multi-layer elastic media corroborate the theoretical analysis.

Keywords: Elastic waves, perfectly matched layer, interface wave modes, stability, Laplace transforms, normal mode analysis

AMS: 65M06, 65M12

1 Introduction

Wave motion is prevalent in many applications and has a great impact on our daily lives. Examples include the use of seismic waves [1, 8] to image natural resources in the Earth's subsurface, to detect cracks and faults in structures, to monitor underground explosions, and to investigate strong ground motions from earthquakes. Most wave propagation problems are formulated in large or infinite domains. However, because of limited computational resources, numerical simulations must be restricted to smaller computational domains by introducing artificial boundaries. Therefore, reliable and efficient domain truncation techniques that significantly minimise artificial reflections are important for the development of effective numerical wave solvers.

A straightforward approach to construct a domain truncation procedure is to surround the computational domain with an absorbing layer of finite thickness such that outgoing waves are absorbed. For this approach to be effective, all outgoing waves entering the layer should decay without reflections, regardless of the frequency and angle of incidence. An absorbing layer with this desirable property is called a perfectly matched layer (PML) [5, 10, 25, 17, 15, 6, 3, 4, 7].

The PML was first derived for electromagnetic waves in the pioneering work [5, 10] but has since then been extended to other applications, for example acoustic and elastic waves [17, 15, 6, 3, 4, 7]. The PML has gained popularity because of its effective absorption properties, versatility, simplicity, ease of derivation and implementation using standard numerical methods. A stable PML model, when effectively implemented in a numerical solver, can yield a domain truncation scheme that ensures the convergence of the numerical solution to the solution of the unbounded problem

*Mathematical Sciences Institute, Australian National University, Australia (kenneth.duru@anu.edu.au).

†Department of Mathematics and Mathematical Statistics, Umeå University, Umeå, Sweden (siyang.wang@umu.se).

[4, 13, 21]. However, the PML is also notorious for supporting fatal instabilities which can destroy the accuracy of numerical solutions. These undesirable exponentially growing modes can be present in both the PML model at the continuous level or numerical methods at the discrete level. The stability analysis of the PML has attracted substantial attention in the literature, see for examples [17, 15, 6, 3, 4, 7], and [19] for a recent review. For hyperbolic PDEs, mode analysis for PML initial value problems (IVP) with constant damping and constant material properties yields a necessary geometric stability condition [6]. When this condition is violated, exponentially growing modes in time are present, rendering the PML model useless. In certain cases, for example the acoustic wave equation with constant coefficients, analytical solutions can be derived [7, 11]. In addition, energy estimates for the PML have recently been derived in physical space [4] and Laplace space [13, 21], which can be useful for deriving stable numerical methods. However, in general, even if the PML IVP does not support growing modes, there can still be stability issues when boundaries and material interfaces are introduced. For the extension of mode stability analysis to boundary and guided waves in homogeneous media, see [17, 14, 15, 18]. The stability analysis of the PML in discontinuous acoustic media was presented in [12]. To the best of our knowledge, the stability analysis of the PML for more general wave media such as the discontinuous or layered elastic solids has not been reported in literature.

In geophysical and seismological applications, the wave media can be composed of layers of rocks, soft and hard sediments, bedrock layers, water and possibly oil. In layered elastic media, the presence of interface wave modes such as Stoneley waves [30, 8], makes the stability analysis of the PML more challenging. Numerical experiments have also reported PML instabilities and poor performance for problems with material boundaries entering into the layer and problems with strong evanescent waves [2]. These existing results have motivated this study to investigate where the inadequacies of the PML arise.

The main objective of this study is to analyse the stability of interface wave modes for the PML in discontinuous elastic solids. Using normal mode analysis, we prove that if the PML IVP has no temporally growing modes, then all interface wave modes present at a planar interface of bi-material elastic solids are dissipated by the PML. The analysis closely follows the steps taken in [17] for boundary waves modes, but here we apply the techniques to investigate the stability of interface wave modes in the PML. Numerical experiments in two-layered isotropic and anisotropic elastic solids, and a multi-layered isotropic elastic solid corroborate the theoretical analysis.

The remainder of the paper proceeds as follows. In the next section, we present the elastic wave equation in discontinuous media, define interface conditions and discuss energy stability for the model problem. In section 3, we introduce the mode analysis for body and interface wave modes, and formulate the determinant condition that is necessary for stability. The PML model is derived in section 4. In section 5, we present the stability analysis of the PML in a piecewise constant elastic medium and formulate the main results. Numerical examples are given in section 6, corroborating the theoretical analysis. In section 7, we draw conclusions.

2 The elastic wave equation in discontinuous media

Consider the 2D elastic wave equation in the two half-planes, $\Omega_1 = (-\infty, \infty) \times (0, \infty)$ and $\Omega_2 = (-\infty, \infty) \times (-\infty, 0)$

$$\rho_i \frac{\partial^2 \mathbf{u}_i}{\partial t^2} = \frac{\partial}{\partial x}\left(A_i \frac{\partial \mathbf{u}_i}{\partial x} + C_i \frac{\partial \mathbf{u_1}}{\partial y}\right) + \frac{\partial}{\partial y}\left(B_i \frac{\partial \mathbf{u}_i}{\partial y} + C_i^T \frac{\partial \mathbf{u}_i}{\partial x}\right), \quad (x, y) \in \Omega_i, \quad i = 1, 2 \tag{1}$$

with a planar interface at $y = 0$ and subject to the smooth initial conditions

$$\mathbf{u}_i(x, y, 0) = \mathbf{f_i}(x, y), \quad \frac{\partial \mathbf{u}_i}{\partial t}(x, y, 0) = \mathbf{g_i}(x, y).$$

At the material interface $y = 0$, we impose physical interface conditions

$$\mathbf{u}_1 = \mathbf{u}_2, \quad B_1 \frac{\partial \mathbf{u}_1}{\partial y} + C_1^T \frac{\partial \mathbf{u}_1}{\partial x} = B_2 \frac{\partial \mathbf{u}_2}{\partial y} + C_2^T \frac{\partial \mathbf{u}_2}{\partial x}, \tag{2}$$

which correspond to continuity of displacement and continuity of traction. For $i = 1, 2$, we have the unknown displacement vectors $\mathbf{u}_i = [u_{i1}, u_{i2}]^T$. The medium parameters are described by the densities $\rho_i > 0$ and the coefficient matrices A_i, B_i, C_i of elastic constants. In 2D orthotropic elastic media, the elastic coefficients are described by four independent parameters c_{11_i}, c_{22_i}, c_{33_i}, c_{12_i} and the coefficient matrices are given by

$$A_i = \begin{bmatrix} c_{11_i} & 0 \\ 0 & c_{33_i} \end{bmatrix}, \quad B_i = \begin{bmatrix} c_{33_i} & 0 \\ 0 & c_{22_i} \end{bmatrix}, \quad C_i = \begin{bmatrix} 0 & c_{12_i} \\ c_{33_i} & 0 \end{bmatrix}, \quad i = 1, 2. \tag{3}$$

Here, the material coefficients c_{11_i}, c_{22_i}, c_{33_i} are always positive, but c_{12_i} may be negative for certain materials. In general, for stability, we require

$$c_{11_i} > 0, \quad c_{22_i} > 0, \quad c_{33_i} > 0, \quad c_{11_i} c_{22_i} - c_{12_i}^2 > 0. \tag{4}$$

For planar waves propagating along the x-direction and $y-$direction, the p-wave speed and s-wave speed are given by

$$c_{px_i} := \sqrt{\frac{c_{11_i}}{\rho_i}}, \quad c_{sx_i} := \sqrt{\frac{c_{33_i}}{\rho_i}}, \quad c_{py_i} := \sqrt{\frac{c_{22_i}}{\rho_i}}, \quad c_{sy_i} := \sqrt{\frac{c_{33_i}}{\rho_i}}. \tag{5}$$

In the case of isotropic media, the material properties can be described by using only two Lamé parameters, $\mu_i > 0$ and λ_i, such that $c_{11_i} = c_{22_i} = 2\mu_i + \lambda_i$, $c_{33_i} = \mu_i > 0$, $c_{12_i} = \lambda_i > -\mu_i$, yielding

$$A_i = \begin{bmatrix} 2\mu_i + \lambda_i & 0 \\ 0 & \mu_i \end{bmatrix}, \quad B_i = \begin{bmatrix} \mu_i & 0 \\ 0 & 2\mu_i + \lambda_i \end{bmatrix}, \quad C_i = \begin{bmatrix} 0 & \lambda_i \\ \mu_i & 0 \end{bmatrix}, \quad i = 1, 2, \tag{6}$$

with the wave speeds

$$c_{pi} := \sqrt{\frac{2\mu_i + \lambda_i}{\rho_i}}, \quad c_{si} := \sqrt{\frac{\mu_i}{\rho_i}}. \tag{7}$$

In isotropic media, a wave mode propagates with the same wave speed in all directions.

We introduce the strain-energy matrix

$$P_i = \begin{bmatrix} A_i & C_i \\ C_i^T & B_i \end{bmatrix}. \tag{8}$$

The symmetric strain-energy matrix P_i is positive semi-definite [26]. For $i = 1, 2$, we define the mechanical energy in the medium Ω_i by

$$E_i(t) = \frac{1}{2} \int_{\Omega_i} \left(\rho_i \left(\frac{\partial \mathbf{u}_i}{\partial t} \right)^T \left(\frac{\partial \mathbf{u}_i}{\partial t} \right) + \begin{bmatrix} \frac{\partial \mathbf{u}_i}{\partial x} \\ \frac{\partial \mathbf{u}_i}{\partial y} \end{bmatrix}^T P_i \begin{bmatrix} \frac{\partial \mathbf{u}_i}{\partial x} \\ \frac{\partial \mathbf{u}_i}{\partial y} \end{bmatrix} \right) dxdy. \tag{9}$$

The following theorem states a stability result for the coupled problem, (1) with (2).

Theorem 1 *The elastic wave equation* (1)*, for $i = 1, 2$, subject to the interface condition* (2) *is energy conserving, that is $E_1(t) + E_2(t) = E_1(0) + E_2(0)$ for all $t \geq 0$, where the energy $E_i(t)$ is defined in* (9)*.*

Proof 1 *Multiply* (1) *by $\left(\frac{\partial \mathbf{u}_i}{\partial t}\right)^T$ and integrate over the spatial domain Ω_i, yielding*

$$\int_{\Omega_i} \rho_i \left(\frac{\partial \mathbf{u}_i}{\partial t}\right)^T \left(\frac{\partial^2 \mathbf{u}_i}{\partial t^2}\right) dxdy = \int_{\Omega_i} \left[\left(\frac{\partial \mathbf{u}_i}{\partial t}\right)^T \frac{\partial}{\partial x}\left(A_i \frac{\partial \mathbf{u}_i}{\partial x}\right) + \left(\frac{\partial \mathbf{u}_i}{\partial t}\right)^T \frac{\partial}{\partial y}\left(B_i \frac{\partial \mathbf{u}_i}{\partial y}\right)\right.$$
$$\left. + \left(\frac{\partial \mathbf{u}_i}{\partial t}\right)^T \frac{\partial}{\partial x}\left(C_i \frac{\partial \mathbf{u}_i}{\partial y}\right) + \left(\frac{\partial \mathbf{u}_i}{\partial t}\right)^T \frac{\partial}{\partial y}\left(C_i^T \frac{\partial \mathbf{u}_i}{\partial x}\right)\right] dxdy.$$

Integrating by parts and summing contributions from both half-planes, $i = 1, 2$, we obtain

$$\sum_{i=1}^{2} \int_{\Omega_i} \rho_i \left(\frac{\partial \mathbf{u}_i}{\partial t}\right)^T \left(\frac{\partial^2 \mathbf{u}_i}{\partial t^2}\right) dxdy = -\sum_{i=1}^{2} \int_{\Omega_i} \left[\left(\frac{\partial^2 \mathbf{u}_i}{\partial t \partial x}\right)^T \left(A_i \frac{\partial \mathbf{u}_i}{\partial x}\right) + \left(\frac{\partial^2 \mathbf{u}_i}{\partial t \partial y}\right)^T \left(B_i \frac{\partial \mathbf{u}_i}{\partial y}\right)\right.$$
$$\left. + \left(\frac{\partial^2 \mathbf{u}_i}{\partial t \partial x}\right)^T \left(C_i \frac{\partial \mathbf{u}_i}{\partial y}\right) + \left(\frac{\partial^2 \mathbf{u}_i}{\partial t \partial y}\right)^T \left(C_i^T \frac{\partial \mathbf{u}_i}{\partial x}\right)\right] dxdy$$
$$- \int_{-\infty}^{\infty} \left(\frac{\partial \mathbf{u}_1}{\partial t}\right)^T \left(B_1 \frac{\partial \mathbf{u}_1}{\partial y} + C_1^T \frac{\partial \mathbf{u}_1}{\partial x}\right)\Big|_{y=0} dx + \int_{-\infty}^{\infty} \left(\frac{\partial \mathbf{u}_2}{\partial t}\right)^T \left(B_2 \frac{\partial \mathbf{u}_2}{\partial y} + C_2^T \frac{\partial \mathbf{u}_2}{\partial x}\right)\Big|_{y=0} dx.$$

The interface terms at $y = 0$ vanish because of (2)*. The relation can then be rewritten as*

$$\frac{1}{2}\frac{d}{dt} \sum_{i=1}^{2} \int_{\Omega_i} \rho_i \left(\frac{\partial \mathbf{u}_i}{\partial t}\right)^T \left(\frac{\partial \mathbf{u}_i}{\partial t}\right) dxdy = -\frac{1}{2}\frac{d}{dt} \sum_{i=1}^{2} \int_{\Omega_i} \begin{bmatrix} \frac{\partial \mathbf{u}_i}{\partial x} \\ \frac{\partial \mathbf{u}_i}{\partial y} \end{bmatrix}^T \begin{bmatrix} A_i & C_i \\ C_i^T & B_i \end{bmatrix} \begin{bmatrix} \frac{\partial \mathbf{u}_i}{\partial x} \\ \frac{\partial \mathbf{u}_i}{\partial y} \end{bmatrix} dxdy.$$

Moving all terms to the left-hand side and identifying the energy gives

$$\frac{d}{dt}\left(E_1(t) + E_2(t)\right) = 0.$$

The time derivative of the energy vanishes, thus $E_1(t) + E_2(t) = E_1(0) + E_2(0)$ for all $t \geq 0$. The proof is complete.

We say that the problem is energy-stable if the energy is conserving or dissipating.

3 Mode analysis

Theorem 1 proves energy stability of the elastic wave equation (1) in general media Ω_i, for $i = 1, 2$, subject to the interface condition (2). However, the theorem does not provide information about the wave modes that may exist in the medium. In this section, we use mode analysis to gain insights on the existence of possible wave modes. More precisely, we start by considering a constant-coefficient problem for the existence of body waves. After that, we analyse interface waves in media with piecewise constant material property and formulate a stability result in the framework of normal mode analysis.

3.1 Plane waves and dispersion relations

To study the existence of body wave modes, we consider the problem (1) in the whole real plane $(x, y) \in \mathbb{R}^2$ with constant medium parameters,

$$\rho_i = \rho, \quad A_i = A, \quad B_i = B, \quad C_i = C,$$

for Ω_i, $i = 1, 2$. In this case, there is no interface condition at $y = 0$, and the material parameters are constant in the entire domain $\Omega_1 \cup \Omega_2$.

Consider the wave-like solution

$$\mathbf{u}\,(x, y, t) = \mathbf{u}_0 e^{st + \boldsymbol{i}(k_x x + k_y y)}, \quad \mathbf{u}_0 \in \mathbb{R}^2, \quad k_x, k_y, x, y \in \mathbb{R}, \quad t \geq 0, \quad \boldsymbol{i} = \sqrt{-1}. \tag{10}$$

In (10), $\mathbf{k} = (k_x, k_y) \in \mathbb{R}^2$ is the wave vector, and $\mathbf{u}_0 \in \mathbb{R}^2$ is a vector of constant amplitude called the polarization vector. By inserting (10) into (1), we have the eigenvalue problem

$$-s^2 \mathbf{u}_0 = \mathscr{P}(\mathbf{k}) \mathbf{u}_0, \quad \mathscr{P}(\mathbf{k}) = \frac{k_x^2 A + k_y^2 B + k_x k_y (C + C^T)}{\rho}. \tag{11}$$

The polarisation vector $\mathbf{u}_0 \in \mathbb{R}^2$ is an eigenvector of the matrix $\mathscr{P}(\mathbf{k})$ and $-s^2$ is the corresponding eigenvalue. For problems that are energy conserving, the matrix $\mathscr{P}(\mathbf{k})$ is symmetric positive definite for all $\mathbf{k} \in \mathbb{R}^2$. Thus, the eigenvectors $\mathbf{u}_0$ of $\mathscr{P}(\mathbf{k})$ are orthogonal and the eigenvalues are real and positive, $-s^2 > 0$.

The wave-mode (10) is a solution of the elastic wave equation (1) in the whole plane $(x, y) \in \mathbb{R}^2$ if s and $\mathbf{k}$ satisfy the dispersion relation

$$F\,(s, \mathbf{k}) := \det\left(s^2 I + \mathscr{P}(\mathbf{k})\right) = 0. \tag{12}$$

Evaluating the determinant and simplifying further, we obtain

$$F\,(s, \mathbf{k}) = s^4 + \frac{(c_{11} + c_{33})\,k_x^2 + (c_{22} + c_{33})\,k_y^2}{\rho} s^2 + \frac{c_{11} c_{33} k_x^4 + c_{22} c_{33} k_y^4 + \left(c_{11} c_{22} + c_{33}^2 - (c_{33} + c_{12})^2\right) k_x^2 k_y^2}{\rho^2} = 0. \tag{13}$$

In an isotropic medium, with $c_{11} = c_{22} = 2\mu + \lambda$, $c_{33} = \mu > 0$, $c_{12} = \lambda > -\mu$, the dispersion relation simplifies to

$$F\,(s, \mathbf{k}) = \left(s^2 + c_p^2 |\mathbf{k}|^2\right)\left(s^2 + c_s^2 |\mathbf{k}|^2\right) = 0, \quad c_p = \sqrt{\frac{2\mu + \lambda}{\rho}}, \quad c_s = \sqrt{\frac{\mu}{\rho}}, \quad |\mathbf{k}| = \sqrt{k_x^2 + k_y^2}. \tag{14}$$

Then, the eigenvalues are given by

$$-s_1^2 = c_p^2 |\mathbf{k}|^2, \quad -s_2^2 = c_s^2 |\mathbf{k}|^2, \tag{15}$$

which correspond to the P-wave and S-wave propagating in the medium. In linear orthotropic elastic media, the eigenvalues $-s^2$ also have closed form expressions

$$\begin{aligned}
-s_1^2 &= \frac{1}{2\rho}\left((c_{11} + c_{33}) k_x^2 + (c_{22} + c_{33}) k_y^2\right) \\
&\quad + \frac{1}{2\rho}\sqrt{\left((c_{11} + c_{33}) k_x^2 + (c_{22} + c_{33}) k_y^2\right)^2 - 4\left(\left(c_{11} c_{33} k_x^4 + c_{22} c_{33} k_y^4\right) + \left(c_{11} c_{22} + c_{33}^2 - (c_{12} + c_{33})^2 k_x^2 k_y^2\right)\right)}, \\
-s_2^2 &= \frac{1}{2\rho}\left((c_{11} + c_{33}) k_x^2 + (c_{22} + c_{33}) k_y^2\right) \\
&\quad - \frac{1}{2\rho}\sqrt{\left((c_{11} + c_{33}) k_x^2 + (c_{22} + c_{33}) k_y^2\right)^2 - 4\left(\left(c_{11} c_{33} k_x^4 + c_{22} c_{33} k_y^4\right) + \left(c_{11} c_{22} + c_{33}^2 - (c_{12} + c_{33})^2 k_x^2 k_y^2\right)\right)}.
\end{aligned} \tag{16}$$

Using the stability conditions (4), it is easy to check that the two eigenvalues are strictly positive, that $-s_j^2 > 0$ for $j = 1, 2$. These two eigenvalues again indicate two body-wave modes, corresponding to the quasi-P waves and the quasi-S waves.

Remark 1 *The indeterminate $s \in \mathbb{C}$ that solves the dispersion relation* (12) *is related to the temporal frequency. Since Theorem 1 holds for all stable medium parameters, the whole plane problem* (1) *conserves energy. Thus, the real part of the roots s must be zero, that is $s \in \mathbb{C}$ with* $\mathrm{Re}\{s\} = 0$*. Otherwise, if the roots s have non-zero real parts then the energy will grow or decay, contradicting Theorem 1.*

We write $s = \boldsymbol{i}\omega$, where $\omega \in \mathbb{R}$ is called the temporal frequency, and introduce

$$\begin{aligned}
\mathbf{K} &= \left(\frac{k_x}{|\mathbf{k}|}, \frac{k_y}{|\mathbf{k}|}\right), \quad \text{normalized propagation direction,} \\
\mathbf{V}_p &= \left(\frac{\omega}{k_x}, \frac{\omega}{k_y}\right), \quad \text{phase velocity,} \\
\mathbf{S} &= \left(\frac{k_x}{\omega}, \frac{k_y}{\omega}\right), \quad \text{slowness vector,} \\
\mathbf{V}_g &= \left(\frac{\partial\omega}{\partial k_x}, \frac{\partial\omega}{\partial k_y}\right), \quad \text{group velocity.}
\end{aligned} \tag{17}$$

For the Cauchy problem in a constant coefficient medium, the dispersion relation $F(i\omega, \mathbf{k}) = 0$ and the quantities $\mathbf{K}$, $\mathbf{V}_p$, $\mathbf{S}$, $\mathbf{V}_g$, defined above give detailed description of the wave propagation properties in the medium. In addition, they determine a stability property for the corresponding PML model, which is discussed in section 5.1. In Figure **??**, we plot the dispersion relations of two different elastic solids, showing the slowness diagrams.

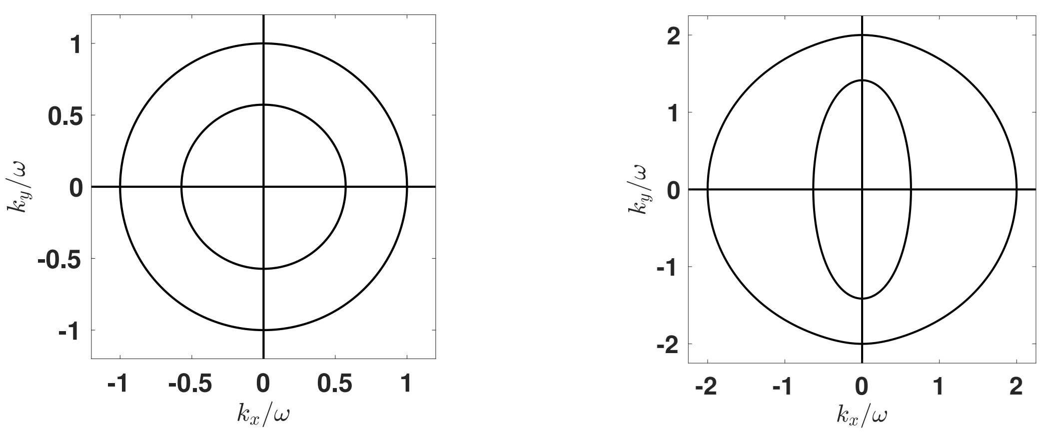

(a) Isotropic elastic solid

(b) Anisotropic elastic solid

When boundaries and interfaces are present, additional boundary and interface wave modes, such as Rayleigh [29] and Stoneley waves [30, 8], are introduced. In the following, we consider the problem in two half-planes coupled together at a planar interface and formulate an alternative procedure to characterise the stability property of interface wave modes.

3.2 Normal modes analysis and the determinant condition

Here, we present the normal modes analysis for interface wave modes in discontinuous media, which tightly connects to the analysis of the PML in the next section. To begin, we consider piecewise constant media parameters

$$\rho_i > 0, \quad A_i, \quad B_i, \quad C_i,$$

for Ω_i, $i=1,2$, where A_i, B_i, C_i are given in (3). The material parameters are constant in each half-plane, but are discontinuous at the interface $y=0$, where the equations (1) are coupled by the interface condition (2). We look for wave solutions in the form

$$\mathbf{u}_i\,(x,y,t) = \boldsymbol{\phi}_i(y)e^{st+\boldsymbol{i}k_x x}, \quad \|\boldsymbol{\phi}_i\| < \infty, \quad k_x \in \mathbb{R}, \quad (x,y) \in \Omega_i, \quad t \geq 0. \tag{18}$$

The variable s is related to the stability property of the model, which is characterised in the following lemma.

Lemma 1 *The elastic wave equations* (1) *with piecewise constant media parameters* (3) *and the interface condition* (2) *are not stable in any sense if there are nontrivial solutions of the form* (18) *with* $\mathrm{Re}\{s\} > 0$.

If there are nontrivial solutions of the form (18), we can always construct solutions that grow arbitrarily fast [17], which is not supported by a stable system. Now, we reformulate Lemma (1) as an algebraic condition, i.e. the so-called determinant condition in Laplace space [23].

For a complex number $z = a + \boldsymbol{i}b$, we define the branch of $\sqrt{z}$ by

$$-\pi < \arg\,(a+\boldsymbol{i}b) \leq \pi, \quad \arg\,(\sqrt{a+\boldsymbol{i}b}) = \frac{1}{2}\arg\,(a+\boldsymbol{i}b).$$

We insert (18) in the equation (1) and the interface condition (2), and obtain

$$s^2\rho_i\boldsymbol{\phi}_i = -k_x^2 A_i\boldsymbol{\phi}_i + B_i\frac{d^2\boldsymbol{\phi}_i}{dy^2} + \boldsymbol{i}k_x\left(C_i + C_i^T\right)\frac{d\boldsymbol{\phi}_i}{dy}, \quad i=1,2, \tag{19}$$

$$\boldsymbol{\phi}_1 = \boldsymbol{\phi}_2, \quad B_1\frac{d\boldsymbol{\phi}_1}{dy} + \boldsymbol{i}k_x C_1^T\boldsymbol{\phi}_1 = B_2\frac{d\boldsymbol{\phi}_2}{dy} + \boldsymbol{i}k_x C_2^T\boldsymbol{\phi}_2. \tag{20}$$

For $\boldsymbol{\phi}_i$, we seek the modal solution

$$\boldsymbol{\phi}_i = \boldsymbol{\Phi}_i e^{\kappa y}, \quad \boldsymbol{\Phi}_i \in \mathbb{C}^2, \quad i=1,2. \tag{21}$$

Inserting the modal solution (21) in (19), we have the eigenvalue problem

$$-s^2\boldsymbol{\Phi}_i = \mathscr{P}_i(k_x,\kappa)\boldsymbol{\Phi}_i, \quad \mathscr{P}_i(k_x,\kappa) = \frac{k_x^2 A_i - \kappa^2 B_i - \boldsymbol{i}k_x\kappa(C_i + C_i^T)}{\rho_i}, \quad i=1,2. \tag{22}$$

The solutions satisfy the condition

$$F_i\,(s,k_x,\kappa) := \det\left(s^2 I + \mathscr{P}_i(k_x,\kappa)\right) = 0. \tag{23}$$

We note that if we set $\kappa = \boldsymbol{i}k_y$ in $F_i\,(s,k_x,\kappa)$, we get exactly the same dispersion relation (12) for the Cauchy problem.

For s with large $\mathrm{Re}\{s\} > 0$, the roots κ_i come in pairs and have non-vanishing real parts, [17], with

$$\kappa_{ij}^-(s,k_x), \quad \kappa_{ij}^+(s,k_x), \quad j=1,2. \tag{24}$$

The following lemma states an important property of the roots.

Lemma 2 *The real parts of the roots* $\kappa_{ij}^{\pm}$, $i,j=1,2$ *in* (24) *do not change sign for all* s *with* $\mathrm{Re}\{s\} > 0$.

Proof 2 *We note that the roots vary continuously with* s*. Thus, if the real part of a root* κ_{ij} *changes sign, then for some* s *with* $\mathrm{Re}\{s\} > 0$ *the root is purely imaginary,* $\kappa_{ij} = \boldsymbol{i}k_y$*. Because of the equivalence between the dispersion relations* (23) *and* (12) *when* $\kappa_{ij} = \boldsymbol{i}k_y$*, a purely imaginary root corresponds to an exponentially growing mode for the Cauchy problem, which contradicts Theorem 1.*

We use the notation (24) to denote the roots with the stated sign convention for all s with $\mathrm{Re}\{s\} > 0$. That is, the superscript $(+)$ denotes the root with positive real part and the superscript $(-)$ denotes the root with negative real part. Because of the condition $\|\boldsymbol{\phi}_i\| < \infty$, the general solution of (19) takes the form

$$\boldsymbol{\phi}_1(y) = \delta_{11}e^{\kappa_{11}^{-}y}\Phi_{11} + \delta_{12}e^{\kappa_{12}^{-}y}\Phi_{12}, \quad \boldsymbol{\phi}_2(y) = \delta_{21}e^{\kappa_{21}^{+}y}\Phi_{21} + \delta_{22}e^{\kappa_{22}^{+}y}\Phi_{22}, \tag{25}$$

where $\Phi_{ij},\ i,j = 1,2$ are the corresponding eigenvectors. As an example, in isotropic linear elastic media, the analytical expressions of the roots and eigenvectors are

$$\kappa_{i1}^{\pm} = \pm\sqrt{k_x^2 + \frac{s^2}{c_{si}^2}}, \quad \kappa_{i2}^{\pm} = \pm\sqrt{k_x^2 + \frac{s^2}{c_{pi}^2}}, \quad i = 1,2,$$

and

$$\Phi_{11} = \begin{bmatrix} \frac{\boldsymbol{i}}{k_x}\kappa_{11}^{-} \\ 1 \end{bmatrix}, \quad \Phi_{12} = \begin{bmatrix} \frac{-\boldsymbol{i}k_x}{\kappa_{12}^{-}} \\ 1 \end{bmatrix}, \quad \Phi_{21} = \begin{bmatrix} \frac{\boldsymbol{i}}{k_x}\kappa_{21}^{+} \\ 1 \end{bmatrix}, \quad \Phi_{22} = \begin{bmatrix} \frac{-\boldsymbol{i}k_x}{\kappa_{22}^{+}} \\ 1 \end{bmatrix}.$$

For orthotropic elastic media, the roots can also be expressed in closed form, but the expressions are much more complicated. We refer the reader to [17] for more details.

The coefficients $\boldsymbol{\delta} = [\delta_{11}, \delta_{12}, \delta_{21}, \delta_{22}]^T$ are determined by inserting (25) into the interface conditions (20), yielding the following equation

$$\mathscr{C}(s, k_x)\boldsymbol{\delta} = \mathbf{0}, \tag{26}$$

where the 4×4 boundary matrix $\mathscr{C}$ takes the form

$$\mathscr{C}(s, k_x) = \begin{bmatrix} \Phi_{11} & \Phi_{12} & -\Phi_{21} & -\Phi_{22} \\ (\kappa_{11}^{-}B_1 + \boldsymbol{i}k_xC_1^T)\Phi_{11} & (\kappa_{21}^{-}B_1 + \boldsymbol{i}k_xC_1^T)\Phi_{12} & -(\kappa_{12}^{+}B_2 + \boldsymbol{i}k_xC_2^T)\Phi_{21} & -(\kappa_{22}^{+}B_2 + \boldsymbol{i}k_xC_2^T)\Phi_{22} \end{bmatrix}. \tag{27}$$

To ensure only trivial solutions for $\mathrm{Re}\{s\} > 0$, the coefficients $\boldsymbol{\delta}$ must vanish, and thus we require the *determinant condition*

$$\mathscr{F}(s, k_x) := \det\left(\mathscr{C}(s, k_x)\right) \neq 0, \quad \forall\, \mathrm{Re}\{s\} > 0. \tag{28}$$

We will now formulate an algebraic definition of stability equivalent to Lemma 1, for the coupled problem, (1) and (2), with piecewise constant media parameters (3).

Lemma 3 *The solutions of the elastic wave equation* (1) *with piecewise constant media parameters* (3) *and the interface condition* (2) *are not stable in any sense if for some* $k_x \in \mathbb{R}$ *and* $s \in \mathbb{C}$ *with* $\mathrm{Re}\{s\} > 0$*, we have*

$$\mathscr{F}(s, k_x) := \det\left(\mathscr{C}(s, k_x)\right) = 0.$$

The *determinant condition* is defined for all s with $\text{Re}\{s\} > 0$. The case when $\text{Re}\{s\} = 0$ would correspond to time-harmonic and important interface wave modes, such as Stoneley waves [23, 24].

The energy stability in Theorem 1 states that the coupled problem, (1) and (2), with piecewise constant media parameters (3) conserves energy. Therefore, similar to Remark 1, the roots s of $\mathscr{F}(s, k_x)$ must be zero or purely imaginary, i.e. $s \in \mathbb{C}$ with $\text{Re}\{s\} = 0$. We conclude that all nontrivial and stable interface wave modes, such as Stoneley waves, that solve $\mathscr{F}(s, k_x) = 0$, must have purely imaginary roots, $s = \boldsymbol{i}\xi$ with $\xi \in \mathbb{R}$. A main objective of the present work is to determine how the purely imaginary roots $s = \boldsymbol{i}\xi$ will move in the complex plane when the PML is introduced.

4 The perfectly matched layer

We consider the elastic wave equation (1) with the interface conditions (2). Let the Laplace transform, in time, of $\mathbf{u}(x, y, t)$ be defined by

$$\widehat{\mathbf{u}}(x, y, s) = \int_0^\infty e^{-st}\mathbf{u}(x, y, t)\,\text{dt}, \quad s = a + \boldsymbol{i}b, \quad \text{Re}\{s\} = a > 0. \tag{29}$$

We consider a setup where the PML is included in the x-direction only. Without loss of generality, we assume that we are only interested in the solution in the left half-plane $x \leq 0$. To absorb outgoing waves, we introduce a PML outside the left half-plane and require that the material properties are invariant in x in PML.

To derive the PML model, we Laplace transform (1) in time, and obtain

$$\rho_i s^2 \widehat{\mathbf{u}}_\mathbf{i} = \frac{\partial}{\partial x}\left(A_i \frac{\partial \widehat{\mathbf{u}}_i}{\partial x}\right) + \frac{\partial}{\partial y}\left(B_i \frac{\partial \widehat{\mathbf{u}}_i}{\partial y}\right) + \frac{\partial}{\partial x}\left(C_i \frac{\partial \widehat{\mathbf{u}}_i}{\partial y}\right) + \frac{\partial}{\partial y}\left(C_i^T \frac{\partial \widehat{\mathbf{u}}_i}{\partial x}\right), \quad (x, y) \in \Omega_i, \quad \text{Re}\{s\} > 0. \tag{30}$$

Note that we have tacitly assumed homogeneous initial data. Next, we consider (30) in the transformed coordinate $(\widetilde{x}, y)$, such that

$$\frac{d\widetilde{x}}{dx} = 1 + \frac{\sigma(x)}{\alpha + s} =: S_x. \tag{31}$$

Here, $\sigma(x) \geq 0$ is the damping function and $\alpha \geq 0$ is the complex frequency shift (CFS) [25]. For all s, we have $S_x \neq 0$ and $1/S_x \neq 0$, and the smooth complex coordinate transformation [10],

$$\frac{\partial}{\partial x} \to \frac{1}{S_x}\frac{\partial}{\partial x}. \tag{32}$$

The PML model in Laplapce space is

$$s^2 \rho_i \widehat{\mathbf{u}}_i = \frac{1}{S_x}\frac{\partial}{\partial x}\left(\frac{1}{S_x} A_i \frac{\partial \widehat{\mathbf{u}}_i}{\partial x}\right) + \frac{\partial}{\partial y}\left(B_i \frac{\partial \widehat{\mathbf{u}}_i}{\partial y}\right) + \frac{1}{S_x}\frac{\partial}{\partial x}\left(C_i \frac{\partial \widehat{\mathbf{u}}_i}{\partial y}\right) + \frac{\partial}{\partial y}\left(C_i^T \frac{1}{S_x}\frac{\partial \widehat{\mathbf{u}}_i}{\partial x}\right), \quad i = 1, 2, \tag{33}$$

with interface conditions

$$\widehat{\mathbf{u}}_1 = \widehat{\mathbf{u}}_2, \quad B_1 \frac{\partial \widehat{\mathbf{u}}_1}{\partial y} + C_1^T \frac{1}{S_x}\frac{\partial \widehat{\mathbf{u}}_1}{\partial x} = B_2 \frac{\partial \widehat{\mathbf{u}}_2}{\partial y} + C_2^T \frac{1}{S_x}\frac{\partial \widehat{\mathbf{u}}_2}{\partial x}. \tag{34}$$

Choosing the auxiliary variables

$$\widehat{\mathbf{v}}_i = \frac{1}{s + \sigma + \alpha}\frac{\partial \widehat{\mathbf{u}}_i}{\partial x}, \quad \widehat{\mathbf{w}}_i = \frac{1}{s + \alpha}\frac{\partial \widehat{\mathbf{u}}_i}{\partial y}, \quad \widehat{\mathbf{q}}_i = \frac{\alpha}{s + \alpha}\widehat{\mathbf{u}}_i,$$

we invert the Laplace transformed equation (33) and obtain the PML model in physical space,

$$
\begin{aligned}
\rho_i \left(\frac{\partial^2 \mathbf{u}_i}{\partial t^2} + \sigma \frac{\partial \mathbf{u}_i}{\partial t} - \sigma\alpha(\mathbf{u}_i - \mathbf{q}_i)\right) &= \frac{\partial}{\partial x}\left(A_i \frac{\partial \mathbf{u}_i}{\partial x} + C_i \frac{\partial \mathbf{u}_i}{\partial y} - \sigma A_i \mathbf{v}_i\right) + \frac{\partial}{\partial y}\left(B_i \frac{\partial \mathbf{u}_i}{\partial y} + C_i^T \frac{\partial \mathbf{u}_i}{\partial x} + \sigma B_i \mathbf{w}_i\right),\\
\frac{\partial \mathbf{v}_i}{\partial t} &= -(\sigma+\alpha)\mathbf{v}_i + \frac{\partial \mathbf{u}_i}{\partial x},\\
\frac{\partial \mathbf{w}_i}{\partial t} &= -\alpha \mathbf{w}_i + \frac{\partial \mathbf{u}_i}{\partial y},\\
\frac{\partial \mathbf{q}_i}{\partial t} &= \alpha(\mathbf{u}_i - \mathbf{q}_i).
\end{aligned}
\tag{35}
$$

Similarly, inverting the Laplace transformed interface conditions (34) for the PML model gives

$$
\mathbf{u_1} = \mathbf{u_2}, \quad B_1 \frac{\partial \mathbf{u_1}}{\partial y} + C_1^T \frac{\partial \mathbf{u_1}}{\partial x} + \sigma B_1 \mathbf{w_1} = B_2 \frac{\partial \mathbf{u_2}}{\partial y} + C_2^T \frac{\partial \mathbf{u_2}}{\partial x} + \sigma B_2 \mathbf{w_2}. \tag{36}
$$

In the absence of the PML, $\sigma = 0$, the above model problem is energy-stable in the sense of Theorem 1 for all elastic material parameters. When $\sigma > 0$, however, the coupled PML model (35)-(36) is asymmetric with auxiliary differential equations. Thus, a similar energy-stability cannot be established in general. To analyse the stability property of the PML model in a piecewise constant elastic medium, we use the mode analysis discussed in Section 3 to prove that exponentially growing wave modes are not supported.

5 Stability analysis of the PML model

The stability analysis of the PML will mirror directly the mode analysis described in Section 3. We will split the analysis into two parts: plane wave analysis for the Cauchy PML problem and normal modes analysis for the interface wave modes.

5.1 Plane waves analysis

We now investigate the stability of body wave modes in the PML in the whole real plane $(x, y) \in \mathbb{R}^2$ with constant medium parameters. As before, we consider constant PML damping $\sigma > 0$ and uniformly constant coefficients medium parameters

$$
\rho_i = \rho, \quad A_i = A, \quad B_i = B, \quad C_i = C,
$$

for Ω_i, $i = 1, 2$, that is there is no discontinuity of material parameters at the interface at $y = 0$.

Consider the wave-like solution

$$
\mathbf{u}\,(x, y, t) = \mathbf{u}_0 e^{st + \boldsymbol{i}(k_x x + k_y y)}, \quad \mathbf{u}_0 \in \mathbb{R}^8, \quad k_x, k_y, x, y \in \mathbb{R}, \quad t \geq 0, \tag{37}
$$

where $s \in \mathbb{C}$ is to be determined and relates to the stability property of the PML model.

Lemma 4 *The PML model* (35) *is not stable if there are nontrivial solutions* $\mathbf{u}$ *of the form* (37) *with* $\mathrm{Re}\{s\} > 0$.

An s with a positive real part, $\mathrm{Re}\{s\} > 0$ corresponds to a plane wave solution with exponentially growing amplitude. A stable system does not admit such wave modes.

We consider the normalised wave vector $\mathbf{K} = (k_1, k_2)$, with $\sqrt{k_1^2 + k_2^2} = 1$ and the normalised variables

$$\lambda = \frac{s}{|\mathbf{k}|}, \quad \epsilon = \frac{\sigma}{|\mathbf{k}|}, \quad \nu = \frac{\alpha}{|\mathbf{k}|}, \quad S_x(\lambda, \epsilon, \nu) = 1 + \frac{\epsilon}{\lambda + \nu}.$$

Thus, if there are $\mathrm{Re}\{\lambda\} > 0$, the PML is unstable.

We insert the plane wave solution (37) in the PML and obtain the dispersion relation

$$F_\epsilon(\lambda, \mathbf{K}) := F\left(\lambda, \frac{1}{S_x(\lambda, \epsilon, \nu)} k_1, k_2\right) = 0, \tag{38}$$

where the function $F(\lambda, \mathbf{K})$ is defined by (13) and (14). The scaled eigenvalue λ is a root of the complicated nonlinear dispersion relation $F_\epsilon(\lambda, \mathbf{K})$ for the PML and defined in (38). When the PML damping vanishes, $\epsilon = 0$ we have $S_x = 1$, and $F_0(\lambda, \mathbf{K}) \equiv F(\lambda, \mathbf{K})$. As shown in Section 3.1, the roots of $F(\lambda, \mathbf{K})$ are purely imaginary and correspond to the body wave modes propagating in a homogeneous elastic medium. When the PML damping is present $\epsilon > 0$, the roots λ can be difficult to determine. However, standard perturbation arguments yield the following well-known result [16, 6, 3].

Theorem 2 (Necessary condition for stability) *Consider the constant coefficient PML, with $\epsilon > 0$, $\nu \geq 0$. Let the elastic medium be described by the phase velocity $\mathbf{V}_p = (V_{px}, V_{py})$ and the group velocity $\mathbf{V}_g = (V_{gx}, V_{gy})$ defiend in (17). If $V_{px}V_{gx} < 0$, then at all sufficiently high frequencies, $|\mathbf{k}| \to \infty$, there are corresponding unstable wave modes with* $\mathrm{Re}\{\lambda\} > 0$.

For the elastic subdomains Ω_i, $i = 1, 2$, we will consider only media parameters where the *geometric stability condition*, $V_{px}V_{gx} > 0$, is satisfied and there no growing modes for the Cauchy PML problem. In particular, it can be shown for isotropic elastic materials that body wave modes inside the PML are asymptotically stable for all frequencies [15, 17]. In many anisotropic elastic materials the geometric stability condition and the complex frequency shift $\alpha > 0$ will ensure the stability of plane wave modes for all frequencies [3]. Next, we will characterise the stability of interface wave modes in the PML.

5.2 Stability analysis of interface wave modes

As above, we assume constant PML damping $\sigma \geq 0$ and piecewise constant elastic media parameters with a planar interface at $y = 0$. We Laplace transform (35)–(36) in time, perform a Fourier transformation in the spatial variable x of (35)–(36) and eliminate all PML auxiliary variables. We have

$$\rho_i s^2 \widetilde{\mathbf{u}}_i = -\widetilde{k}_x^2 A_i \widetilde{\mathbf{u}}_i + B_i \frac{\mathrm{d}^2 \widetilde{\mathbf{u}}_i}{\mathrm{d}y^2} + \boldsymbol{i}\widetilde{k}_x \left(C_i + C_i^T\right) \frac{\mathrm{d}\widetilde{\mathbf{u}}_i}{\mathrm{d}y}, \quad i = 1, 2, \tag{39}$$

where $\widetilde{k}_x = k_x / S_x$. The Laplace-Fourier transformed interface conditions are

$$\widetilde{\mathbf{u}}_\mathbf{1} = \widetilde{\mathbf{u}}_\mathbf{2}, \quad B_1 \frac{\mathrm{d}\widetilde{\mathbf{u}}_\mathbf{1}}{\mathrm{d}y} + \boldsymbol{i}\widetilde{k}_x C_1^T \widetilde{\mathbf{u}}_\mathbf{1} = B_2 \frac{\mathrm{d}\widetilde{\mathbf{u}}_\mathbf{2}}{\mathrm{d}y} + \boldsymbol{i}\widetilde{k}_x C_2^T \widetilde{\mathbf{u}}_\mathbf{2}, \quad y = 0. \tag{40}$$

Note the similarity between (39)–(40) and (19)–(20); the only difference is that we have replaced k_x with $\widetilde{k}_x$ and $\boldsymbol{\phi}_i$ with $\widetilde{\mathbf{u}}_i$. When the PML damping vanishes $\sigma = 0$, we have $S_x \equiv 1$ and $\widetilde{k}_x \equiv k_x$. In this case, the PML model (39)–(40) is equivalent to the original equation (19)–(20), and (39) is the Laplace-Fourier transformations of equation (1).

We seek modal solutions to (39) in the form

$$\widetilde{\mathbf{u}}_i = \boldsymbol{\Phi}_i e^{\kappa y}, \quad \boldsymbol{\Phi}_i \in \mathbb{C}^2, \quad i = 1, 2. \tag{41}$$

Substituting (41) into (39), we obtain

$$\left(s^2 I + \mathscr{P}_i(\widetilde{k}_x, \kappa)\right) \mathbf{\Phi}_i = 0, \quad i = 1, 2, \tag{42}$$

where

$$\mathscr{P}_i(\widetilde{k}_x, \kappa) = \widetilde{k}_x^2 A_i - \kappa^2 B_i - \boldsymbol{i}\widetilde{k}_x \kappa (C_i + C_i^T), \quad i = 1, 2.$$

The existence of nontrivial solutions to (42) requires that

$$F_i\left(s, \widetilde{k}_x, \kappa\right) := \det\left(s^2 I + \mathscr{P}_i(\widetilde{k}_x, \kappa)\right) = 0, \quad i = 1, 2. \tag{43}$$

As above, we note that if we set $\kappa = \boldsymbol{i}k_y$ in $F_i\,(s, k_x, \kappa)$, we get exactly the same PML dispersion relation (38) for the Cauchy problem. Again, note also the close similarity between (23) and (43). The roots, $\kappa = \widetilde{\kappa}_{ij}^{\pm}$, of the characteristic function $F_i\left(s, \widetilde{k}_x, \kappa\right)$ are

$$\widetilde{\kappa}_{ij}^{-}(s, k_x) = \kappa_{ij}^{-}(s, \widetilde{k}_x), \quad \widetilde{\kappa}_{ij}^{+}(s, k_x) = \kappa_{ij}^{+}(s, \widetilde{k}_x), \quad j = 1, 2.$$

For the proceeding analysis to directly mirror the mode analysis discussed in section 3.2, we will need the sign consistency between $\mathrm{Re}\left\{\kappa_{ij}^{\pm}\right\}$ and $\mathrm{Re}\left\{\widetilde{\kappa}_{ij}^{\pm}\right\}$. That is for $\mathrm{Re}\{s\} > 0$, $\sigma \geq 0$ and $\alpha \geq 0$ we must have

$$\mathrm{sign}\left(\mathrm{Re}\left\{\kappa_{ij}^{\pm}\right\}\right) = \mathrm{sign}\left(\mathrm{Re}\left\{\widetilde{\kappa}_{ij}^{\pm}\right\}\right). \tag{44}$$

The following lemma, which uses a standard continuity argument, was first proven in [17].

Lemma 5 *If the PML Cauchy problem has no temporally growing modes, then for all $k_x \in \mathbb{R}$ and all $s \in \mathbb{C}$ with $\mathrm{Re}\{s\} > 0$ the PML characteristic equation has roots $\widetilde{\kappa}_{ij}^{\pm}(s, k_x)$ with*

$$\mathit{sign}\left(\mathrm{Re}\left\{\kappa_{ij}^{\pm}\right\}\right) = \mathit{sign}\left(\mathrm{Re}\left\{\widetilde{\kappa}_{ij}^{\pm}\right\}\right).$$

Proof 3 *As above, we note that the roots vary continuously with s. Thus, if the real part of a root $\widetilde{\kappa}_{ij}$ changes sign, then for some s with $\mathrm{Re}\{s\} > 0$ the root must be purely imaginary, $\widetilde{\kappa}_{ij} = \boldsymbol{i}k_y$. When $\kappa_{ij} = \boldsymbol{i}k_y$ the PML dispersion relations (38) for the Cauchy problem and the characteristic (43) are equivalent. Therefore a purely imaginary root $\kappa_{ij} = \boldsymbol{i}k_y$ with $\mathrm{Re}\{s\} > 0$ corresponds to an exponentially growing mode for the Cauchy PML problem, which contradicts the assumption that the Cauchy PML problem has no growing wave modes.*

Taking into account the boundedness condition, the general solution of (39) is

$$\widetilde{\mathbf{u}}_{\mathbf{1}}(y) = \delta_{11} e^{\widetilde{\kappa}_{11}^{-} y} \Phi_{11} + \delta_{12} e^{\widetilde{\kappa}_{12}^{-} y} \Phi_{12}, \quad \widetilde{\mathbf{u}}_{\mathbf{2}}(y) = \delta_{21} e^{\widetilde{\kappa}_{21}^{+} y} \Phi_{21} + \delta_{22} e^{\widetilde{\kappa}_{22}^{+} y} \Phi_{22}, \tag{45}$$

The coefficients $\boldsymbol{\delta} = [\delta_{11}, \delta_{12}, \delta_{21}, \delta_{22}]^T$ are determined by inserting (45) into the interface conditions (20). We have the following equation

$$\mathscr{C}(s, \widetilde{k}_x)\boldsymbol{\delta} = \mathbf{0}, \tag{46}$$

where

$$\mathscr{C}(s, \widetilde{k}_x) = \begin{bmatrix} \Phi_{11} & \Phi_{12} & -\Phi_{21} & -\Phi_{22} \\ (\widetilde{\kappa}_{11}^{-} B_1 + \boldsymbol{i}\widetilde{k}_x C_1^T)\Phi_{11} & (\widetilde{\kappa}_{21}^{-} B_1 + \boldsymbol{i}\widetilde{k}_x C_1^T)\Phi_{12} & -(\widetilde{\kappa}_{12}^{+} B_2 + \boldsymbol{i}\widetilde{k}_x C_2^T)\Phi_{21} & -(\widetilde{\kappa}_{22}^{+} B_2 + \boldsymbol{i}\widetilde{k}_x C_2^T)\Phi_{22} \end{bmatrix}. \tag{47}$$

Using the determinant condition given in Definition 3, we formulate a stability condition for the PML in a piecewise constant elastic medium.

Lemma 6 (Stability condition) *The solution to the PML model* (39) *with piecewise constant material parameters* (3) *and interface condition* (40) *is not stable in any sense if for some $k_x \in \mathbb{R}$ and $s \in \mathbb{C}$ with $\mathrm{Re}\{s\} > 0$, the determinant vanishes,*

$$\mathscr{F}(s, \widetilde{k}_x) := \det\left(\mathscr{C}(s, \widetilde{k}_x)\right) = 0.$$

The roots of $\mathscr{F}(s, \widetilde{k}_x)$ are tightly connected to the roots of $\mathscr{F}(s, k_x)$ by the homogeneous property of $\mathscr{F}$. As a consequence, it is enough to analyse the roots of $\mathscr{F}(s, k_x)$ for the stability property of the PML model. Below, we define the homogeneous property, followed by a theorem for the PML stability.

Definition 1 *Let $\boldsymbol{f}(\boldsymbol{v})$ be a function with the vector argument $\boldsymbol{v}$. If $\boldsymbol{f}(\alpha \boldsymbol{v}) = \alpha^n \boldsymbol{f}(\boldsymbol{v})$ for all $\alpha \neq 0$ and some $n \in \mathbb{Z}$, then $\boldsymbol{f}(\boldsymbol{v})$ is homogeneous of degree n.*

Theorem 3 *Let $\mathscr{F}(s, k_x)$ be a homogeneous function of degree n. Assume that $\mathscr{F}(s, k_x) \neq 0$ for all $\mathrm{Re}\{s\} > 0$ and $k_x \in \mathbb{R}$. Let $\widetilde{k}_x = k_x/S_x$, where S_x is the PML metric* (31). *Then the function $\mathscr{F}(s, \widetilde{k}_x)$ has no root s with positive real part, $\mathrm{Re}\{s\} > 0$.*

Proof 4 *Consider the homogeneous function $\mathscr{F}(s, k_x)$, we have*

$$\mathscr{F}(s, \widetilde{k}_x) = \mathscr{F}\left(s, \frac{k_x}{S_x}\right) = \left(\frac{1}{S_x}\right)^n \mathscr{F}\left(sS_x, k_x\right).$$

Since $S_x \neq 0$ and $1/S_x \neq 0$, we must have

$$\mathscr{F}(s, \widetilde{k}_x) = 0 \iff \mathscr{F}\left(\widetilde{s}, k_x\right) = 0, \quad \widetilde{s} = sS_x.$$

Assume that $s = a + \boldsymbol{i}b$ with $a > 0$, we have

$$\mathrm{Re}\{\widetilde{s}\} = \left(a + \left(\frac{a\,(a+\alpha) + b^2}{|s+\alpha|^2}\right)\sigma\right) \geq a > 0.$$

Thus if $\mathscr{F}\left(\widetilde{s}, k_x\right) = 0$ then $\widetilde{s}$ with $\mathrm{Re}\{\widetilde{s}\} > 0$ is a root. This will contradict the assumption that $\mathscr{F}\left(s, k_x\right) \neq 0$ for all $\mathrm{Re}\{s\} > 0$. We conclude that for $s = a + \boldsymbol{i}b$ with $a > 0$, we must have $\mathscr{F}\left(\widetilde{s}, k_x\right) \neq 0$ for all $\sigma \geq 0$ and $\alpha \geq 0$.

To determine the homogeneity property of $\mathscr{F}(s, k_x) = \det(\mathscr{C}(s, k_x))$, we may evaluate the corresponding determinant of $\mathscr{C}(s, k_x)$. We have the following result.

Theorem 4 *In a piecewise isotropic medium, the determinant $\mathscr{F}(s, k_x) = \det\left(\mathscr{C}\left(s, k_x\right)\right)$ given in* (28) *is homogeneous of degree two.*

Proof 5 *Consider the modified boundary matrix $\mathscr{C}_1(s, k_x)$ where we have multiplied the first two rows of $\mathscr{C}(s, k_x)$ by $s \neq 0$, that is*

$$\mathscr{C}_1(s, k_x) = \begin{bmatrix} s\Phi_{11} & s\Phi_{12} & -s\Phi_{21} & -s\Phi_{22} \\ (\kappa_{11}^{-} B_1 + \boldsymbol{i}k_x C_1^T)\Phi_{11} & (\kappa_{21}^{-} B_1 + \boldsymbol{i}k_x C_1^T)\Phi_{12} & -(\kappa_{12}^{+} B_2 + \boldsymbol{i}k_x C_2^T)\Phi_{21} & -(\kappa_{22}^{+} B_2 + \boldsymbol{i}k_x C_2^T)\Phi_{22} \end{bmatrix}. \quad (48)$$

By inspection, every element of $\mathscr{C}_1(s, k_x)$ is homogeneous of degree one. Therefore the determinant $\det(\mathscr{C}_1(s, k_x))$ of the 4×4 matrix $\mathscr{C}_1(s, k_x)$, using cofactor expansion, must be homogeneous of degree four. Note that

$$\mathscr{C}_1(s, k_x) = \mathscr{K}(s)\mathscr{C}(s, k_x), \quad \mathscr{K}(s) = \begin{bmatrix} s & 0 & 0 & 0 \\ 0 & s & 0 & 0 \\ 0 & 0 & 1 & 0 \\ 0 & 0 & 0 & 1 \end{bmatrix}.$$

Using the properties of the determinants of products of matrices we have

$$\det(\mathscr{C}_1(s,k_x)) = \det(\mathscr{K}(s))\det(\mathscr{C}(s,k_x)) = s^2\det(\mathscr{C}(s,k_x)) = s^2\mathscr{F}(s,k_x).$$

Since $\det(\mathscr{C}_1(s,k_x))$ *is homogeneous of degree four, therefore the determinant* $\mathscr{F}(s,k_x)$ *is homogeneous of degree two.*

We can now state the result that shows that exponentially growing waves modes are not supported by the PML in a discontinuous elastic medium.

Theorem 5 *Consider the PML* (39) *in a discontinuous elastic medium with the interface condition* (40) *at* $y=0$*. Let* $\mathscr{F}(s,k_x)$ *be the homogeneous function given in* (28)*. If* $\mathscr{F}(s,k_x)\neq 0$ *for all* $\mathrm{Re}\{s\}>0$ *and* $k_x\in\mathbb{R}$ *and the PML Cauchy problem has no temporally growing modes, then there are no growing interface wave modes in the PML. That is* $\mathscr{F}(s,\widetilde{k}_x)\neq 0$ *for all* $\mathrm{Re}\{s\}>0$ *and* $k_x\in\mathbb{R}$*.*

Proof 6 *The proof is identical to the proof of Theorem 3 with degree of homogeneity* $n=2$*.*

The following theorem states that interface wave modes are dissipated by the PML.

Theorem 6 *Consider the PML* (39) *in a discontinuous elastic medium with the interface condition* (40) *at* $y=0$*. If the PML Cauchy problem has no temporally growing modes then all stable interface wave modes, that solve* $\mathscr{F}(s,k_x)=0$ *for all* $k_x\in\mathbb{R}$ *with* $s=\boldsymbol{i}\xi$*, are dissipated by the PML.*

Proof 7 *It suffices to prove that* $\mathscr{F}(s,\widetilde{k}_x)=0$ *implies* $\mathrm{Re}\{s\}\leq 0$ *for all* $k_x\in\mathbb{R}$*,* $\alpha\geq 0$ *and* $\sigma\geq 0$*. We will split the proof into two cases, for* $\alpha=0$ *and* $\alpha>0$*.*

When $\alpha=0$*, we have*

$$\mathscr{F}(s,\widetilde{k}_x)=0 \iff \mathscr{F}(\widetilde{s},k_x)=0, \quad \widetilde{s}=sS_x=\frac{\alpha+s+\sigma}{\alpha+s}s.$$

Since $\mathscr{F}(s_0,k_x)$ *has purely imaginary roots* $s_0=\boldsymbol{i}\xi$*, we must have*

$$\frac{\alpha+s+\sigma}{\alpha+s}s=\boldsymbol{i}\xi, \tag{49}$$

for some $\xi\in\mathbb{R}$*. Thus, if* $\alpha=0$*, then* $s=-\sigma+\boldsymbol{i}\xi$ *and* $\mathrm{Re}\{s\}=-\sigma<0$*.*

When $\alpha>0$*, we consider*

$$\frac{\alpha+s+\sigma}{\alpha+s}s=\boldsymbol{i}\xi \iff s^2+(\alpha+\sigma-\boldsymbol{i}\xi)s-\boldsymbol{i}\alpha\xi=0.$$

If $\xi=0$*, then the roots are* $s=0$ *and* $s=-(\alpha+\sigma)<0$*. Clearly the real parts of the roots are non-positive. If* $\xi\neq 0$*, then the roots are given by*

$$s=-\frac{(\alpha+\sigma-\boldsymbol{i}\xi)}{2}\pm\frac{1}{2}\sqrt{(\alpha+\sigma-\boldsymbol{i}\xi)^2+\boldsymbol{i}4\alpha\xi}.$$

The real parts of the two roots are

$$\mathrm{Re}\{s\}=-\frac{(\alpha+\sigma)}{2}\pm\frac{1}{2\sqrt{2}}\sqrt{(\alpha+\sigma)^2-\xi^2+\sqrt{((\alpha+\sigma)^2-\xi^2)^2+4\xi^2(\alpha-\sigma)^2}}.$$

We note that the root with a negative sign has a negative real part,

$$\operatorname{Re}\{s\} = -\frac{(\alpha+\sigma)}{2} - \frac{1}{2\sqrt{2}}\sqrt{(\alpha+\sigma)^2 - \xi^2 + \sqrt{((\alpha+\sigma)^2-\xi^2)^2 + 4\xi^2(\alpha-\sigma)^2}} < 0.$$

For the other root with a positive sign,

$$\operatorname{Re}\{s\} = -\frac{(\alpha+\sigma)}{2} + \frac{1}{2\sqrt{2}}\sqrt{(\alpha+\sigma)^2 - \xi^2 + \sqrt{((\alpha+\sigma)^2-\xi^2)^2 + 4\xi^2(\alpha-\sigma)^2}},$$

if we assume that $\operatorname{Re}\{s\} > 0$ *for* $\alpha > 0$, $\sigma > 0$ *and* $\xi \in \mathbb{R}$, *then this implies that*

$$(\alpha+\sigma) < \frac{1}{\sqrt{2}}\sqrt{(\alpha+\sigma)^2 - \xi^2 + \sqrt{((\alpha+\sigma)^2-\xi^2)^2 + 4\xi^2(\alpha-\sigma)^2}}.$$

Squaring both sides of the inequality gives

$$(\alpha+\sigma)^2 + \xi^2 < \sqrt{((\alpha+\sigma)^2-\xi^2)^2 + 4\xi^2(\alpha-\sigma)^2}.$$

Squaring both sides again and simplifying further yields

$$(\alpha+\sigma)^2 < (\alpha-\sigma)^2.$$

This is a contradiction since $\alpha > 0$ *and* $\sigma > 0$. *Thus, for* $\alpha > 0$ *and* $\sigma > 0$, *we must have* $\operatorname{Re}\{s\} < 0$. *The roots are moved further by the PML into the stable complex plane.*

6 Numerical experiments

In this section, we present some numerical examples to verify the stability analysis performed in the previous sections and demonstrate the absorption properties of the PML model for the elastic wave equation with piecewise constant material parameters.

6.1 Two layers

We consider the elastic wave equation in a two-layered medium $\Omega_1 \cup \Omega_2$, where $\Omega_1 = [0, 4\pi]^2$ and $\Omega_2 = [0, 4\pi] \times [-4\pi, 0]$. The material property in each layer is either isotropic or orthotropic anisotropic elastic solid. For the isotropic case, we use the material parameters $\rho_1 = 1.5$, $\mu_1 = 4.86$, $\lambda_1 = 4.8629$ in Ω_1, and $\rho_2 = 3$, $\mu_2 = 27$, $\lambda_2 = 26.9952$ in Ω_2. For the anisotropic material property, we choose $\rho_1 = 1$, $c_{11_1} = 4$, $c_{12_1} = 3.8$, $c_{22_1} = 20$ and $c_{33_1} = 2$ in Ω_1, and the material parameters in Ω_2 are chosen as $\rho_2 = 0.25$ and $c_{ij_2} = 4c_{ij_1}$ for $i, j = 1, 2$.

For initial conditions, we set the initial displacements as

$$\mathbf{u_1} = \mathbf{u_2} = e^{-20((\mathbf{x}-2\pi)^2+(\mathbf{y}-1.6\pi)^2)},$$

and zero initial data for the velocity field and all auxiliary variables. We impose the transformed interface conditions (36) at the material interface $y = 0$. We impose characteristic boundary conditions at the left boundary $x = 0$, the bottom boundary $y = -4\pi$, and the top boundary $y = 4\pi$. Outside the right boundary $x = 4\pi$, we use a PML $[4\pi, 4.4\pi] \times [-4\pi, 4\pi]$ closed by the characteristic boundary condition at the PML boundaries. Because of the PML, the boundary conditions must be modified as

$$Z_{1y}\frac{\partial \mathbf{u_1}}{\partial t}+B_1\frac{\partial \mathbf{u_1}}{\partial y}+C_1^T\frac{\partial \mathbf{u_1}}{\partial x}+B_1\sigma\mathbf{w_1}+\sigma Z_{1y}(\mathbf{u_1}-\mathbf{q_1})=0,\quad y=4\pi, \tag{50}$$

$$Z_{ix}\frac{\partial \mathbf{u}_i}{\partial t}-A_i\frac{\partial \mathbf{u}_i}{\partial x}-C_i\frac{\partial \mathbf{u}_i}{\partial y}+A_i\sigma\mathbf{v_i}=0,\quad x=0,\ \mathbf{i}=1,2, \tag{51}$$

$$Z_{ix}\frac{\partial \mathbf{u}_i}{\partial t}+A_i\frac{\partial \mathbf{u}_i}{\partial x}+C_i\frac{\partial \mathbf{u}_i}{\partial y}-A_i\sigma\mathbf{v_i}=0,\quad x=4.4\pi,\ \mathbf{i}=1,2, \tag{52}$$

$$Z_{2y}\frac{\partial \mathbf{u_2}}{\partial t}-B_2\frac{\partial \mathbf{u_2}}{\partial y}-C_2^T\frac{\partial \mathbf{u_2}}{\partial x}-B_2\sigma\mathbf{w_2}+\sigma Z_{2y}(\mathbf{u_2}-\mathbf{q_2})=0,\quad y=-4\pi. \tag{53}$$

The impedance matrices Z_{ix} and Z_{iy} are given by

$$Z_{ix}=\begin{bmatrix}\rho_i c_{pxi} & 0\\ 0 & \rho_i c_{sxi}\end{bmatrix},\quad Z_{iy}=\begin{bmatrix}\rho_i c_{syi} & 0\\ 0 & \rho_i c_{pyi}\end{bmatrix},$$

and the wave speeds $c_{pxi}, c_{pyi}, c_{sxi}, c_{syi}$ are defined in (5).

The PML damping function is

$$\sigma(x)=\begin{cases} 0 & \text{if} \quad x\le L_x,\\ \sigma_0\left(\frac{x-L_x}{\delta}\right)^3 & \text{if} \quad x\ge L_x,\end{cases} \tag{54}$$

where the damping strength is

$$\sigma_0=\frac{4c_{p,\max}}{2\delta}\log\left(\frac{1}{Ref}\right). \tag{55}$$

Here, $c_{p,\max}=\max(c_{p1},c_{p2})$, $c_{p1}=\max(c_{px1},c_{py1})$ and $c_{p2}=\max(c_{px2},c_{py2})$ are the maximum pressure wave speeds in Ω_1 and Ω_2, respectively. The parameter $L_x=4\pi$ is the length of the domain, $\delta=0.1L_x$ is the width of the PML and $Ref=10^{-4}$ is the relative PML modeling error. Additionally, we choose the CFS $\alpha=0.05\sigma_0$ in both subdomains.

For the spatial discretisation, we use the SBP finite difference operators with the fourth order accurate interior stencil [28]. The boundary conditions and material interface conditions are imposed weakly by the penalty technique [20, 9] such that a discrete energy estimate is obtained when the damping vanishes. For details on the SBP discretisation and stability for the undamped problem, we refer the reader to [20, 22]. We discretise in time using the classical Runge-Kutta method with the time step $\Delta t=0.2h/\sqrt{\max_i(c_{pi}^2+c_{si}^2)}$. As above $c_{pi}=\max(c_{pxi},c_{pyi})$ are the maximum pressure wave speeds in Ω_i and $c_{si}=\max(c_{sxi},c_{syi})$ are the maximum shear wave speeds in Ω_i.

In Figure 2-3, we plot the numerical solutions at four time points for the isotropic and anisotropic media, respectively. In both cases, the initial data is a Gaussian in the top layer. At $t=1$, we observe that a wave mode propagates at the same speed in the two spatial directions in the isotropic medium but at different speeds in the anisotropic medium. The elastic waves have propagated into the bottom layer at $t=2$, where the effects of discontinuous material property are clearly observed. At $t=5$, it is clear that waves coming into the PML are absorbed. In the last panels, we plot the solution after long time $t=100$. Note that the largest amplitude is about 10^{-5}, demonstrating numerical stability and the effectiveness of PML.

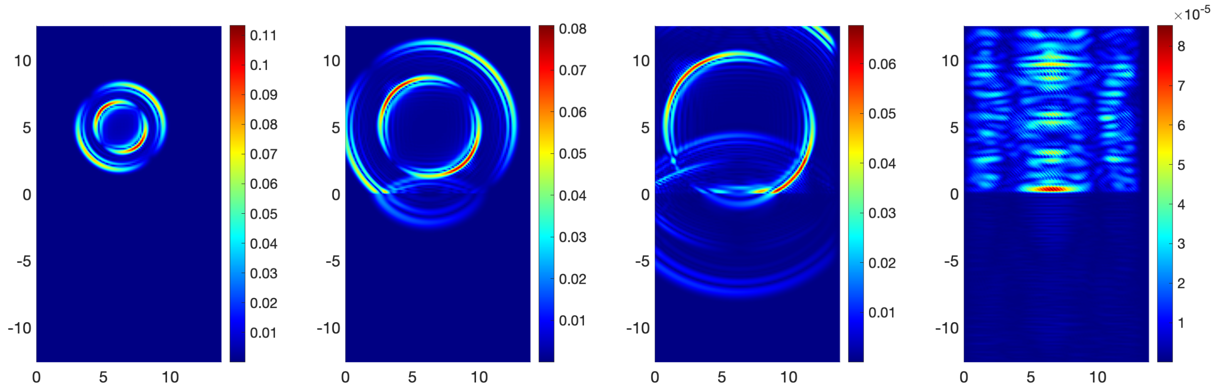

Figure 2: The solution at four time points $t = 1, 2, 3, 100$ in a piecewise isotropic medium.

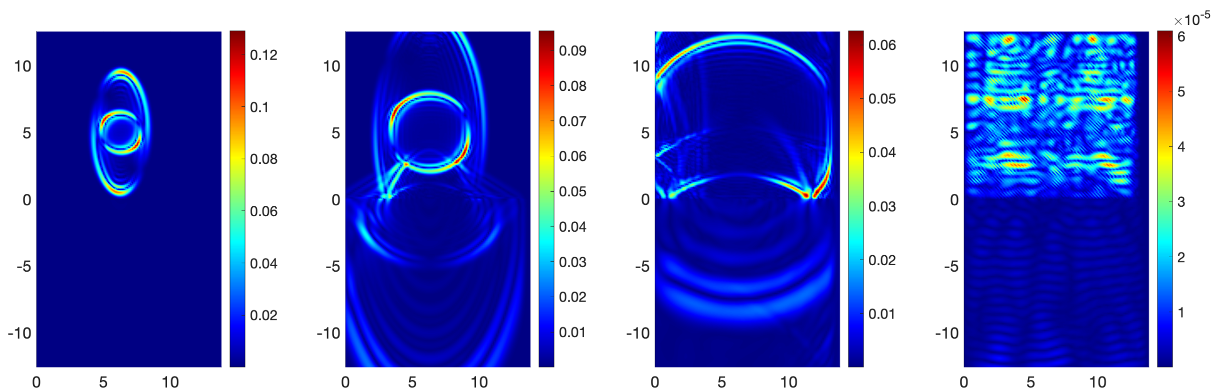

Figure 3: The solution at four time points $t = 1, 2, 5, 100$ in a piecewise orthotropic medium.

In Figure 4, using the computed numerical solution we plot the l_2-norm $\|\mathbf{u}\|_H = \sqrt{\sum_{i=1}^{2} \mathbf{u}_i^T \mathbf{H} \mathbf{u}_i}$ in time, where i corresponds to the two layers and $\mathbf{H}$ the discrete norm associated with the SBP operator. We observe that $\|\mathbf{u}\|_H$ decays monotonically in both the isotropic and anisotropic media.

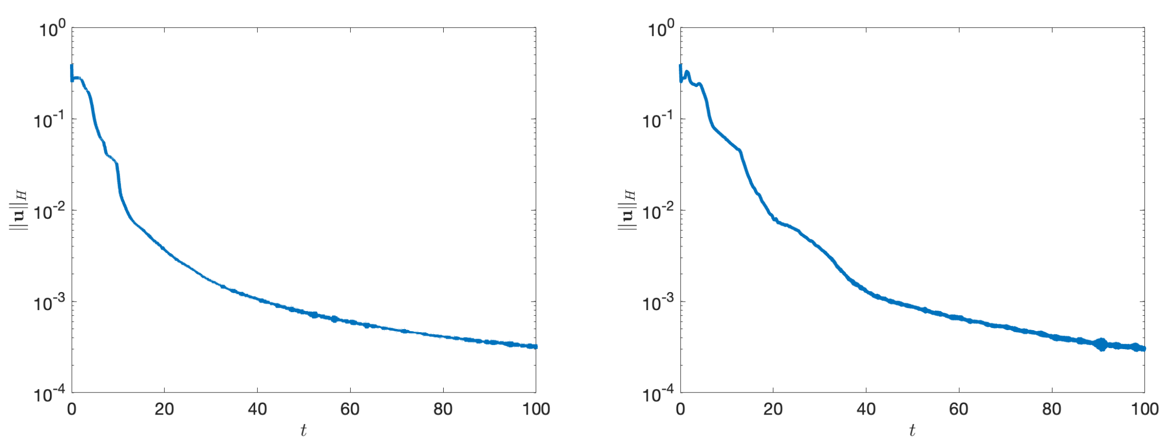

Figure 4: The quantity $\|\mathbf{u}\|_H$ with for the isotropic (left) and the orthotropic (right) media.

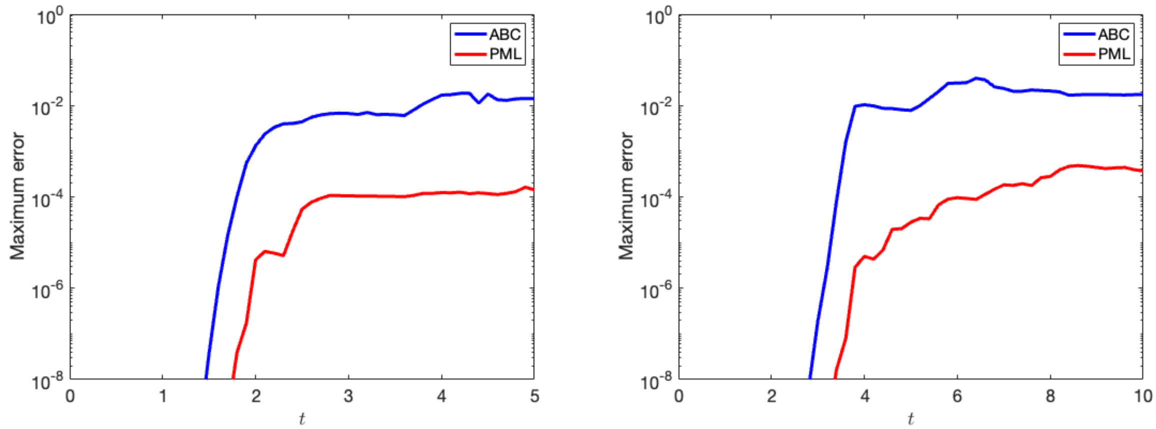

Figure 5: The maximum error for the isotropic (left) and the orthotropic (right) media. ABC is absorbing boundary condition.

Layer	ρ	c_s	c_p	Domain
1	1.5	1.8	3.118	$[0, 40] \times [-10, 0]$
2	1.9	2.3	3.984	$[0, 40] \times [-20, -10]$
3	2.1	2.7	4.667	$[0, 40] \times [-30, -20]$
4	3	3	5.196	$[0, 40] \times [-40, -30]$

Table 1: Material properties in the four layers.

Finally, we compare the absorbing property of the PML model with the first order absorbing boundary conditions (ABC) [27]. We compute a solution in the large domain $[0, 4\pi] \times [-4\pi, 12\pi]$, which is the original domain extended three times in the positive x direction, and regard the part of the solution in $[0, 4\pi] \times [-4\pi, 4\pi]$ as a reference solution. In Figure 5, we plot the PML error defined as the maximum norm of the difference between the PML solution and the reference solution, and the ABC error that is defined analogously as the maximum norm of the difference between the solution computed by using the ABC on all boundaries and the reference solution. We observe that the PML error is about two order of magnitude smaller than the ABC error in both isotropic and anisotropic media.

6.2 Four layers

Next we demonstrate extension of the results to multiple elastic layers. We consider the elastic wave equation in domain $\Omega = [0, 40] \times [-40, 0]$. The medium has a four-layered structure and the material parameters are summarized in Table 1. In each layer, the material property is homogeneous and isotropic, and the governing equation is (35). At the interface between two adjacent layers, the material property is discontinuous, and the equations are coupled by imposing continuity of displacement and traction in the form of (36). At time $t = 0$, we initialise the displacement fields as

$$\mathbf{u}_i = e^{-5((x-20)^2+(y+15)^2)}, \quad i = 1, 2, 3, 4,$$

that is, a Gaussian centred in the middle of Layer 2.

We impose a traction free boundary condition at the top boundary $y = 0$, and the characteristic boundary condition at the bottom boundary $y = -40$ and the left boundary $x = 0$. At the right boundary $x = 40$, we add a PML in $[40, 44] \times [-40, 0]$, where the width $\delta = 4$ is 10% of the computational domain in x. At the boundaries of the PML, we impose the characteristic boundary condition. Because of the PML, the boundary conditions must be modified as

$$B_1 \frac{\partial \mathbf{u_1}}{\partial y} + C_1^T \frac{\partial \mathbf{u_1}}{\partial x} + B_1 \sigma \mathbf{w_1} = 0, \quad y = 0, \tag{56}$$

$$Z_{ix} \frac{\partial \mathbf{u}_i}{\partial t} - A_i \frac{\partial \mathbf{u}_i}{\partial x} - C_i \frac{\partial \mathbf{u}_i}{\partial y} + A_i \sigma \mathbf{v_i} = 0, \quad x = 0,\ i = 1, 2, 3, 4, \tag{57}$$

$$Z_{ix} \frac{\partial \mathbf{u}_i}{\partial t} + A_i \frac{\partial \mathbf{u}_i}{\partial x} + C_i \frac{\partial \mathbf{u}_i}{\partial y} - A_i \sigma \mathbf{v_i} = 0, \quad x = 44,\ i = 1, 2, 3, 4, \tag{58}$$

$$Z_{4y} \frac{\partial \mathbf{u_4}}{\partial t} - B_4 \frac{\partial \mathbf{u_4}}{\partial y} - C_4^T \frac{\partial \mathbf{u_4}}{\partial x} - B_4 \sigma \mathbf{w_4} + \sigma Z_{4y}(\mathbf{u_4} - \mathbf{q_4}) = 0, \quad y = -40. \tag{59}$$

More precisely, on the y-boundaries the modified traction includes the auxiliary variable $\mathbf{w}$. In addition, the time derivative in the characteristic boundary condition introduces a lower order term, see (59). Similarly, on the x-boundaries, the modified traction includes the auxiliary variable $\mathbf{v}$.

Inside the PML of all four layers, we choose the damping function $\sigma(x)$ is given by (54), where the damping strength $\sigma_0 > 0$ is given by (55). Here, $c_{p,max} = \max_i c_{pi}$ is the largest pressure wave speed c_{pi} in Ω_i, $i = 1, 2, 3, 4$, $L_x = 40$, $\delta = 0.1L_x$, and $Ref = 10^{-4}$ is the relative modeling error. Additionally, we choose the CFS $\alpha = 0.05\sigma_0$.

Numerically, we use the same spatial and temporal discretisation as in the previous numerical example. In Figure 6, we plot the solutions at four time points with grid size $h = 0.1$. We observe that at $t = 3$, the Gaussian has expanded from its centre to the top three layers and the reflections at the material interfaces are clearly visible. At $t = 5$, the wave has propagated to all four layers, and has interacted with the free surface, at $y = 0$, and the characteristic boundary condition, at $x = 0$. The plot at $t = 9$ shows that the surface wave entering the PML is effectively absorbed. After a long time until $t = 1000$, most waves have left the computational domain and the largest amplitude is only 10^{-6}.

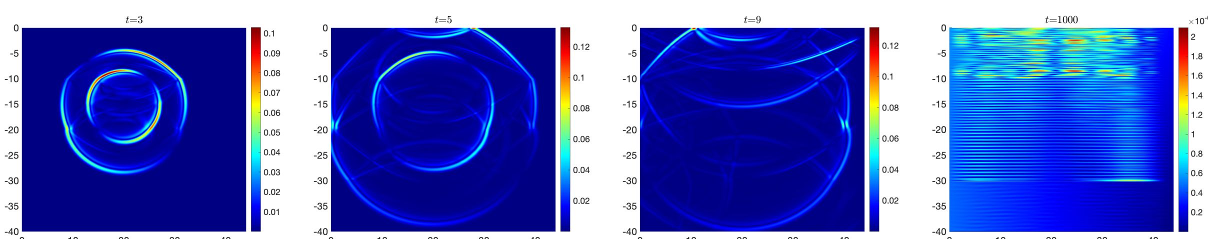

Figure 6: The solution at four time points $t = 3, 5, 9$ and 1000 with Gaussian initial data and grid size $h = 0.1$.

Next, we consider an example driven by seismological sources, an explosive moment tensor point source $F = gM_0\nabla f_\delta$, as the forcing in the governing equation. The moment time function g and the approximated delta function f_δ take the form

$$g = e^{-\frac{(t-0.215)^2}{0.15}}, \quad f_\delta = \frac{1}{2\pi\sqrt{s_1 s_2}} e^{-\left(\frac{(x-20)^2}{2s_1} + \frac{(y+15)^2}{2s_2}\right)},$$

where the parameters $s_1 = s_2 = 0.5h$ and $M_0 = 1000$. We note that the peak amplitude of F is located in the middle of Layer 2. With zero initial data for all variables, we run the simulation until $t = 1000$ using the same numerical method, and plot the solutions by $h = 0.1$ in Figure 7. We have similar observation as the case with a Gaussian initial data.

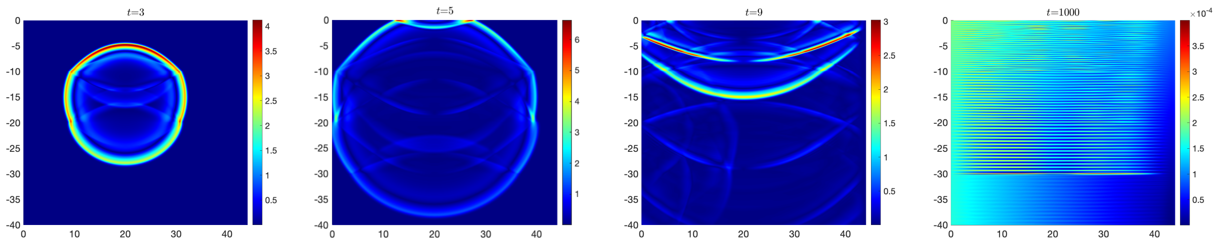

Figure 7: The solution at four time points $t = 3, 5, 9$ and 1000 with single point moment source and grid size $h = 0.1$.

To see the stability property of the PML, we plot $\|\mathbf{u}\|_H$ in time in Figure 8. The first plot correspond to the case with Gaussian initial data, and the second plot corresponds to the case with the single point moment source. It is clear that the PML remains stable after a long time.

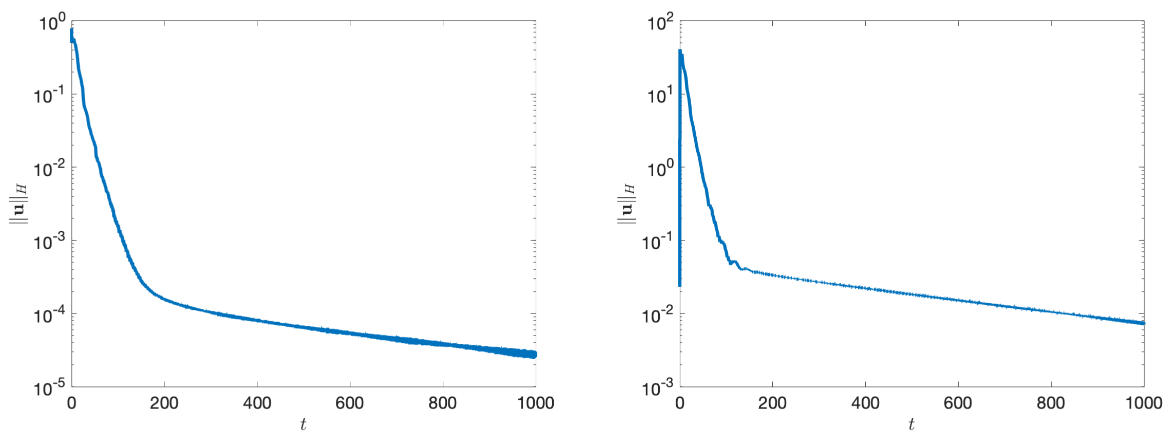

Figure 8: The quantity $\|\mathbf{u}\|_H$ with $h = 0.1$ for the Gaussian initial data (left) and the single point moment source (right).

As before, we compare the absorbing property of the PML model with the ABC. Similar to the last section, we compute a reference solution in a larger domain that is extended in the positive x direction three times the length of the original domain. In all computations, we have used a spatial mesh size $h = 0.2$. In Figure 9, we plot the PML error and the ABC error, and observe again that the PML error is about two orders of magnitude smaller than the ABC error for both cases.

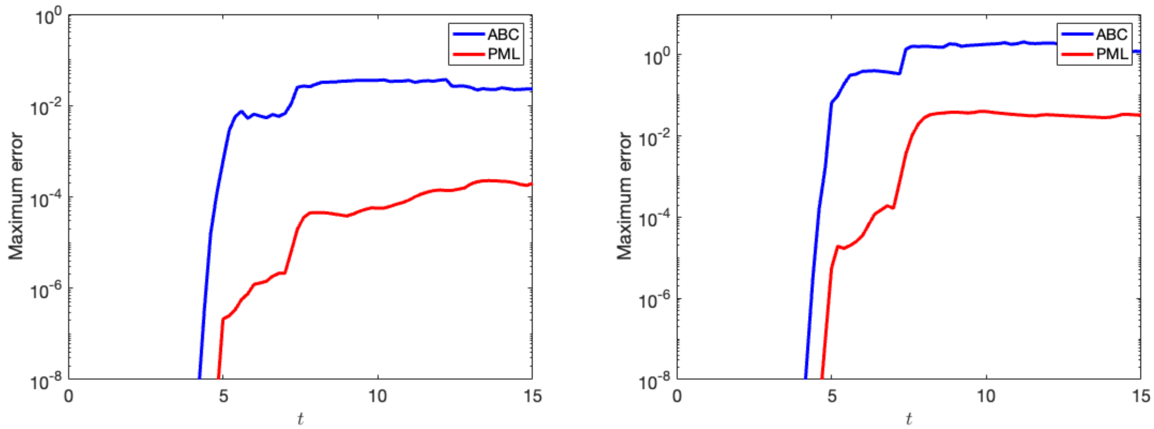

Figure 9: The maximum error for the case with Gaussian initial data (left) and with the single point moment source (right). ABC is absorbing boundary condition.

7 Conclusion

We have analysed the stability of the PML for the elastic wave equation with piecewise constant material parameters and interface conditions at material interfaces. The elastic wave equation and the interface conditions, without the PML, satisfy an energy estimate in physical space. Alternatively, a mode analysis can also be used to prove that exponentially growing modes are not supported by the elastic wave equation subject to the interface conditions. In particular, the normal mode analysis in Laplace space for interface waves gives a boundary matrix $\mathscr{C}(s, k_x)$ of which the determinant is a homogeneous function $\mathscr{F}(s, k_x)$ of (s, k_x) and does not have any roots s with a positive real part $\mathrm{Re}\{s\} > 0$ in the complex plane. When the PML is present, the energy method is in general not applicable but the normal mode analysis can be used to investigate the existence of exponentially growing modes in the PML. The normal mode analysis when applied to the PML in a discontinuous elastic medium yields a similar boundary matrix perturbed by the PML. Our analysis shows that if the PML IVP does not support growing modes, then the PML moves the roots of the determinant $\mathscr{F}(s, k_x)$ further into the stable complex plane. This proves that interface wave modes present at layered material interfaces in elastic solids are dissipated by the PML. We have presented numerical examples for both isotropic and anisotropic elastic solids verifying the analysis, and demonstrating that interface wave modes decay in the PML.

Acknowledgement

Part of the work was carried out during S. Wang's research visit at Australian National University (ANU). The financial support from SVeFUM and ANU is greatly appreciated.

References

[1] K. Aki and P. G. Richards, *Quantitative Seismology*, University Science Books, 2 ed., 2002, `http://www.worldcat.org/isbn/0935702962`.

[2] D. Appelö and T. Colonius, *A high-order super-grid-scale absorbing layer and its application to linear hyperbolic systems*, Journal of Computational Physics, 228 (2009),

pp. 4200–4217, https://doi.org/https://doi.org/10.1016/j.jcp.2009.02.030, https://www.sciencedirect.com/science/article/pii/S0021999109001089.

[3] D. Appelö and G. Kreiss, *A new absorbing layer for elastic waves*, Journal of Computational Physics, 215 (2006), pp. 642–660, https://doi.org/https://doi.org/10.1016/j.jcp.2005.11.006, https://www.sciencedirect.com/science/article/pii/S0021999105005097.

[4] D. H. Baffet, M. J. Grote, S. Imperiale, and M. Kachanovska, *Energy decay and stability of a perfectly matched layer for the wave equation*, Journal of Scientific Computing, 81 (2019), pp. 2237–2270, https://doi.org/https://doi.org/10.1007/s10915-019-01089-9.

[5] J.-P. Berenger, *A perfectly matched layer for the absorption of electromagnetic waves*, Journal of Computational Physics, 114 (1994), pp. 185–200, https://doi.org/https://doi.org/10.1006/jcph.1994.1159, https://www.sciencedirect.com/science/article/pii/S0021999184711594.

[6] E. Bécache, S. Fauqueux, and P. Joly, *Stability of perfectly matched layers, group velocities and anisotropic waves*, Journal of Computational Physics, 188 (2003), pp. 399–433, https://doi.org/https://doi.org/10.1016/S0021-9991(03)00184-0, https://www.sciencedirect.com/science/article/pii/S0021999103001840.

[7] E. Bécache and M. Kachanovska, *Stability and convergence analysis of time-domain perfectly matched layers for the wave equation in waveguides*, SIAM Journal on Numerical Analysis, 59 (2021), pp. 2004–2039, https://doi.org/10.1137/20M1330543, https://doi.org/10.1137/20M1330543, https://arxiv.org/abs/https://doi.org/10.1137/20M1330543.

[8] L. Cagnaird, *Reflection and refraction of progressive seismic waves: by L. Cagnaird, Translated from the French and revised by E. A. Flinn and C. H. Dix. McGraw-Hill Book Co. Inc. 1962*, Bulletin of the Seismological Society of America, 53 (1963), pp. 217–218, https://doi.org/10.1785/BSSA0530010217B, https://doi.org/10.1785/BSSA0530010217B, https://arxiv.org/abs/https://pubs.geoscienceworld.org/ssa/bssa/article-pdf/53/1/217/5348070/bssa0530010217b.pdf.

[9] M. H. Carpenter, D. Gottlieb, and S. Abarbanel, *Time–stable boundary conditions for finite–difference schemes solving hyperbolic systems: methodology and application to high–order compact schemes*, Journal of Computational Physics, 111 (1994), pp. 220–236, https://doi.org/https://doi.org/10.1006/jcph.1994.1057.

[10] W. C. Chew and W. H. Weedon, *A 3d perfectly matched medium from modified maxwell's equations with stretched coordinates*, Microwave and Optical Technology Letters, 7 (1994), pp. 599–604, https://doi.org/https://doi.org/10.1002/mop.4650071304, https://onlinelibrary.wiley.com/doi/abs/10.1002/mop.4650071304, https://arxiv.org/abs/https://onlinelibrary.wiley.com/doi/pdf/10.1002/mop.4650071304.

[11] J. Diaz and P. Joly, *A time domain analysis of pml models in acoustics*, Computer Methods in Applied Mechanics and Engineering, 195 (2006), pp. 3820–3853, https://doi.org/https://doi.org/10.1016/j.cma.2005.02.031, https://www.sciencedirect.com/science/article/pii/S0045782505002604.

[12] K. Duru, *A perfectly matched layer for the time-dependent wave equation in heterogeneous and layered media*, Journal of Computational Physics, 257 (2014), pp. 757–781, https://doi.org/https://doi.org/10.1016/j.jcp.2013.10.022, https://www.sciencedirect.com/science/article/pii/S0021999113006980.

[13] K. Duru, A.-A. Gabriel, and G. Kreiss, *On energy stable discontinuous galerkin spectral element approximations of the perfectly matched layer for the wave equation*, Computer Methods in Applied Mechanics and Engineering, 350 (2019), pp. 898–937, https://doi.org/https://doi.org/10.1016/j.cma.2019.02.036, https://www.sciencedirect.com/science/article/pii/S0045782519301070.

[14] K. Duru, J. E. Kozdon, and G. Kreiss, *Boundary conditions and stability of a perfectly matched layer for the elastic wave equation in first order form*, Journal of Computational Physics, 303 (2015), pp. 372–395, https://doi.org/https://doi.org/10.1016/j.jcp.2015.09.048, https://www.sciencedirect.com/science/article/pii/S0021999115006567.

[15] K. Duru and G. Kreiss, *On the accuracy and stability of the perfectly matched layer in transient waveguides*, Journal of Scientific Computing, 53 (2012), pp. 642–671, https://doi.org/https://doi.org/10.1007/s10915-012-9594-7, https://doi.org/10.1007/s10915-012-9594-7.

[16] K. Duru and G. Kreiss, *A well-posed and discretely stable perfectly matched layer for elastic wave equations in second order formulation*, Communications in Computational Physics, 11 (2012), p. 1643–1672, https://doi.org/10.4208/cicp.120210.240511a.

[17] K. Duru and G. Kreiss, *Boundary waves and stability of the perfectly matched layer for the two space dimensional elastic wave equation in second order form*, SIAM Journal on Numerical Analysis, 52 (2014), pp. 2883–2904, https://doi.org/https://doi.org/10.1137/13093563X.

[18] K. Duru and G. Kreiss, *Numerical interaction of boundary waves with perfectly matched layers in two space dimensional elastic waveguides*, Wave Motion, 51 (2014), pp. 445–465, https://doi.org/https://doi.org/10.1016/j.wavemoti.2013.11.002, https://www.sciencedirect.com/science/article/pii/S0165212513001753.

[19] K. Duru and G. Kreiss, *The perfectly matched layer (PML) for hyperbolic wave propagation problems: A review*, 2022, https://doi.org/10.48550/ARXIV.2201.03733, https://arxiv.org/abs/2201.03733.

[20] K. Duru, G. Kreiss, and K. Mattsson, *Stable and high–order accurate boundary treatments for the elastic wave equation on second–order form*, SIAM Journal on Scientific Computing, 36 (2014), pp. A2787–A2818, https://doi.org/https://doi.org/10.1137/130947210.

[21] K. Duru, L. Rannabauer, A.-A. Gabriel, G. Kreiss, and M. Bader, *A stable discontinuous galerkin method for the perfectly matched layer for elastodynamics in first order form*, Numerische Mathematik, 146 (2020), pp. 729–782, https://doi.org/10.1007/s00211-020-01160-w, https://doi.org/10.1007/s00211-020-01160-w.

[22] K. Duru and K. Virta, *Stable and high order accurate difference methods for the elastic wave equation in discontinuous media*, Journal of Computational Physics, 279 (2014), pp. 37–62, https://doi.org/https://doi.org/10.1016/j.jcp.2014.08.046.

[23] B. Gustafsson, H. O. Kreiss, and J. Oliger, *Time–Dependent Problems and Difference Methods*, John Wiley & Sons, 2013, https://doi.org/DOI:10.1002/9781118548448.

[24] H. O. Kreiss, O. E. Ortiz, and N. A. Petersson, *Initial–boundary value problems for second order systems of partial differential equations*, ESAIM–Mathematical Modelling and Numerical Analysis, 46 (2012), pp. 559–593, https://doi.org/https://doi.org/10.1051/m2an/2011060.

[25] M. Kuzuoglu and R. Mittra, *Frequency dependence of the constitutive parameters of causal perfectly matched anisotropic absorbers*, IEEE Microwave and Guided Wave Letters, 6 (1996), pp. 447–449, https://doi.org/10.1109/75.544545.

[26] W. M. Lai, D. Rubin, and E. Krempl, *Introduction to Continuum Mechanics*, Butterworth-Heinemann, 1993, https://doi.org/https://doi.org/10.1016/B978-0-7506-8560-3.X0001-1.

[27] J. Lysmer and R. L. Kuhlemeyer, *Finite dynamic model for infinite media*, Journal of the Engineering Mechanics Division, 95 (1969), pp. 859–877, https://doi.org/10.1061/JMCEA3.0001144, https://ascelibrary.org/doi/abs/10.1061/JMCEA3.0001144, https://arxiv.org/abs/https://ascelibrary.org/doi/pdf/10.1061/JMCEA3.0001144.

[28] K. Mattsson and J. Nordström, *Summation by parts operators for finite difference approximations of second derivatives*, Journal Computational Physics, 199 (2004), pp. 503–540, https://doi.org/https://doi.org/10.1016/j.jcp.2004.03.001.

[29] L. Rayleigh, *On waves propagated along the plane surface of an elastic solid*, Proceedings of the London Mathematical Society, s1-17 (1885), pp. 4–11, https://doi.org/https://doi.org/10.1112/plms/s1-17.1.4, https://londmathsoc.onlinelibrary.wiley.com/doi/abs/10.1112/plms/s1-17.1.4, https://arxiv.org/abs/https://londmathsoc.onlinelibrary.wiley.com/doi/pdf/10.1112/plms/s1-17.1.4.

[30] R. Stoneley and H. F. Baker, *Elastic waves at the surface of separation of two solids*, Proceedings of the Royal Society of London. Series A, Containing Papers of a Mathematical and Physical Character, 106 (1924), pp. 416–428, https://doi.org/10.1098/rspa.1924.0079, https://royalsocietypublishing.org/doi/abs/10.1098/rspa.1924.0079, https://arxiv.org/abs/https://royalsocietypublishing.org/doi/pdf/10.1098/rspa.1924.0079.